Janus Spectra in Two-Dimensional Flows

Chien-Chia Liu, Rory T. Cerbus, and Pinaki Chakraborty*
Fluid Mechanics Unit, Okinawa Institute of Science and Technology Graduate University, Onna-son, Okinawa, Japan 904-0495

(Received 11 December 2015; published 8 September 2016)

In large-scale atmospheric flows, soap-film flows, and other two-dimensional flows, the exponent of the turbulent energy spectra, α, may theoretically take either of two distinct values, 3 or $5/3$, but measurements downstream of obstacles have invariably revealed $\alpha = 3$. Here we report experiments on soap-film flows where downstream of obstacles there exists a sizable interval in which α transitions from 3 to $5/3$ for the streamwise fluctuations but remains equal to 3 for the transverse fluctuations, as if two mutually independent turbulent fields of disparate dynamics were concurrently active within the flow. This species of turbulent energy spectra, which we term the Janus spectra, has never been observed or predicted theoretically. Our results may open up new vistas in the study of turbulence and geophysical flows.

DOI: 10.1103/PhysRevLett.117.114502

Turbulence sculpts clouds. By examining the ever-changing patterns in rising cumulus clouds, Richardson [1] postulated the concept of an energy cascade: the mean flow supplies turbulent kinetic energy to the large-scale fluctuations, or large eddies, which split to engender smaller eddies, which, in turn, engender even smaller eddies, and so forth. This progressive spawning of smaller eddies cascades the energy from larger to smaller scales. The smallest eddies of the cascade dissipate the energy viscously.

In 1941, Kolmogorov [2] casted the energy cascade in a mathematical form. In this celebrated theory—the phenomenological theory of turbulence—Kolmogorov introduced the notion of local isotropy. Physically, local isotropy is based on the idea that as larger eddies spawn smaller eddies, the smaller eddies progressively lose any sense of orientation. While the large eddies (of size L) are anisotropic, the small eddies (of size $l \ll L$) are isotropic. Assuming local isotropy, Kolmogorov argued that the energy is transferred without dissipation for a range of small eddies, $L \gg l \gg \eta$, where η is the size of the smallest eddies that effect viscous dissipation. These are the eddies of the "inertial range." In the inertial range, the turbulent energy spectrum $E(k)$ takes a self-similar form $E(k) \sim k^{-\alpha}$, where k is the wave number ($k \sim 1/l$) and α the "spectral exponent." Invoking dimensional analysis, the phenomenological theory predicts $\alpha = 5/3$ [3].

Consider two-dimensional turbulent flows. In the 1960s, Kraichnan [4], Leith [5], and Batchelor [6] adapted the phenomenological theory to 2D turbulent flows. This theory predicts two distinct cascades in the locally isotropic small scales. In the "direct enstrophy cascade," enstrophy is transferred without dissipation from larger to smaller scales, and in the "inverse energy cascade," energy is transferred without dissipation from smaller to larger scales, the inverse of the 3D energy cascade.

The cascades can be identified via $E(k)$. In the inertial range, $E(k) \sim k^{-\alpha}$. Each cascade pairs with a specific value of α. Instead of $E(k)$, experiments typically measure a closely related quantity, the one-dimensional turbulent energy spectra [7]: the streamwise energy spectrum $E_{uu}(k_x)$ and the transverse energy spectrum $E_{vv}(k_x)$; u is the streamwise velocity fluctuation, v the transverse velocity fluctuation, x the streamwise direction, and k_x the streamwise

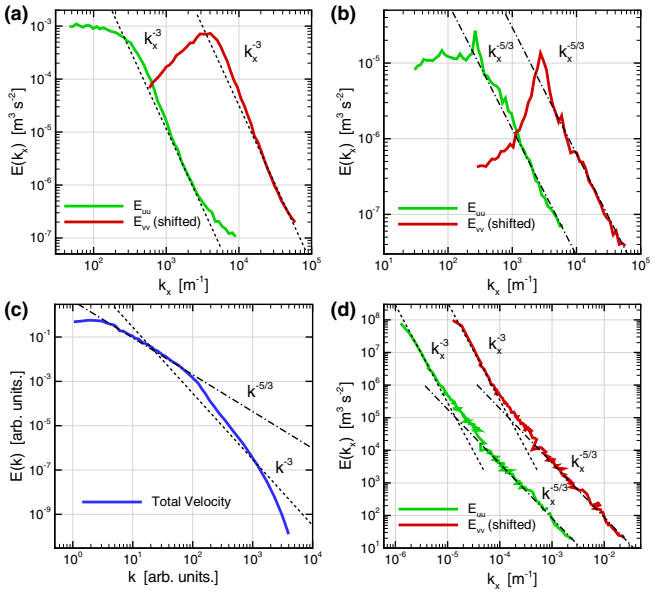

FIG. 1. Log-log plots of typical turbulent energy spectra in 2D turbulence. (a) Direct enstrophy cascade (experimental setup of Ref. [8]). (b) Inverse energy cascade (experimental setup of Ref. [8]). (c) Double cascade (from Ref. [9]; $\alpha = \alpha_u = \alpha_v$ is implicit in this plot; $\alpha > 3$ in the span of the direct enstrophy cascade is attributed to finite-size effects). (d) Atmospheric cascade (from Ref. [10]). Plots of $E_{vv}(k_x)$ (red) are shifted from those of $E_{uu}(k_x)$ (green) for clarity. In all cases, $\alpha_u \approx \alpha_v$.

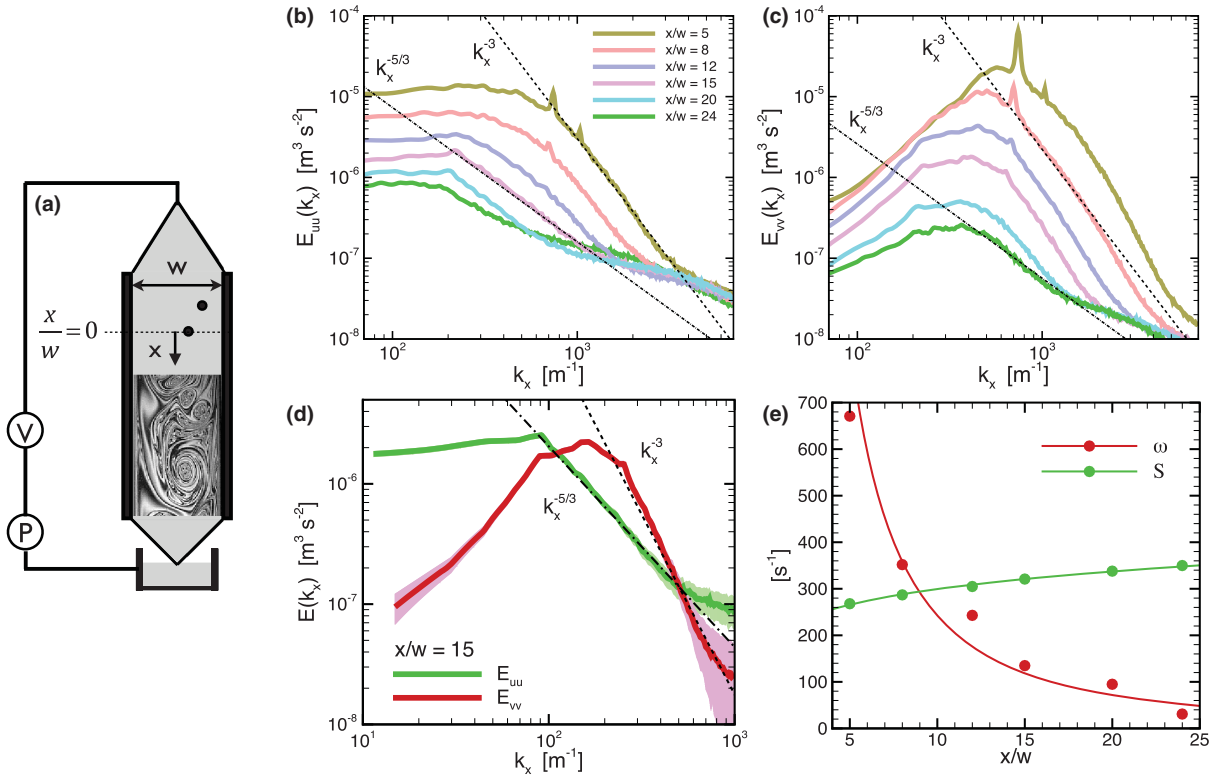

FIG. 2. Route to the Janus spectra in turbulence induced by two rods (also, see the Supplemental Material [14] Fig. S-2). (a) Schematic of the experimental setup [20]. The ≈5 μm thick falling soap film hangs vertically from two steel blades that are 1.6 m long and $w = 12$ mm apart from each other. The soap film is sustained by recirculating a Newtonian soap-water solution (1% commercial detergent in water) via a pump P and through a valve V (to control the flow rate). The soap film is pierced with two rods (of diameter 1 mm, placed 2 and 4 mm transversely away from the center line, and 25 mm vertically staggered from each other). The mean velocity at the center line spans 1.60–2.10 m/s. (b),(c) Evolution of $E_{uu}(k_x)$ and $E_{vv}(k_x)$ with downstream distance. (d) Janus spectra at $x/w = 15$. The shaded regions in $E_{uu}(k_x)$ and $E_{vv}(k_x)$ represent error bars (see the Supplemental Material [14] Sec. S-2). Note that in the inertial region, the errors are negligible. (e) Evolution of turbulent vorticity (ω) and mean shear (S) with downstream distance (see the Supplemental Material [14] Sec. S-3). The best-fit lines are to guide the eye.

wave number. In the inertial range $E_{uu}(k_x) \sim k_x^{-\alpha_u}$ and $E_{vv}(k_x) \sim k_x^{-\alpha_v}$. Local isotropy mandates $\alpha_u = \alpha_v = \alpha$.

Invoking dimensional analysis, the phenomenological theory of 2D turbulence predicts $\alpha = 3$ for the direct enstrophy cascade and $\alpha = 5/3$ for the inverse energy cascade [3]. In Figs. 1(a) and 1(b) we show plots of typical experimental data exhibiting the direct enstrophy cascade and the inverse energy cascade, respectively. These two canonical cascades of 2D turbulence combine to engender two other well-known cascades. In the "double cascade" [Fig. 1(c)], $\alpha = 5/3$ at low k (inverse energy cascade) and $\alpha = 3$ at high k (direct enstrophy cascade). Large-scale atmospheric flows exhibit a transposed variant of the double cascade [Fig. 1(d)].

In all the cases shown in Fig. 1, we note, in accord with local isotropy, $\alpha_u \approx \alpha_v \approx 3$ or $\alpha_u \approx \alpha_v \approx 5/3$. By contrast, here we report experiments on turbulent soap-film flows in which local isotropy is manifestly violated; over a sizable interval of space and over a shared span of wave numbers, we find $\alpha_u \approx 5/3$ (corresponding to the inverse energy cascade) and $\alpha_v \approx 3$ (corresponding to the direct enstrophy cascade). We term this "two-faced" turbulent energy spectra, the Janus spectra (after Janus, the two-faced Roman deity). To our knowledge, any report of such a species of turbulent energy spectra is unprecedented in 2D turbulent flows [11].

Let us briefly consider, for context, the well-studied case of decaying 2D turbulence without a mean flow [12,13]. Here the turbulence decays in time. Initially, the flow exhibits the direct enstrophy cascade, $\alpha_u \approx \alpha_v \approx 3$. Later, the flow evolves to markedly steeper inertial-range energy spectra, $\alpha_u \approx \alpha_v \sim 4$–5. Local isotropy prevails throughout the evolution of the flow.

We conduct experiments in a soap-film channel, a well-known setup for studying quasi-2D turbulent flows [Fig. 2(a)]. To induce turbulence in the soap film, we pierce it with two rods nonsymmetrically about the center line. (This setup emulates an atmospheric flow; see the Supplemental Material [14] Fig. S-1.) The rods shed eddies as the film squeezes past them. The eddies render the flow turbulent, which decays downstream of the rods. A decaying 2D turbulent flow is a canonical case for the direct

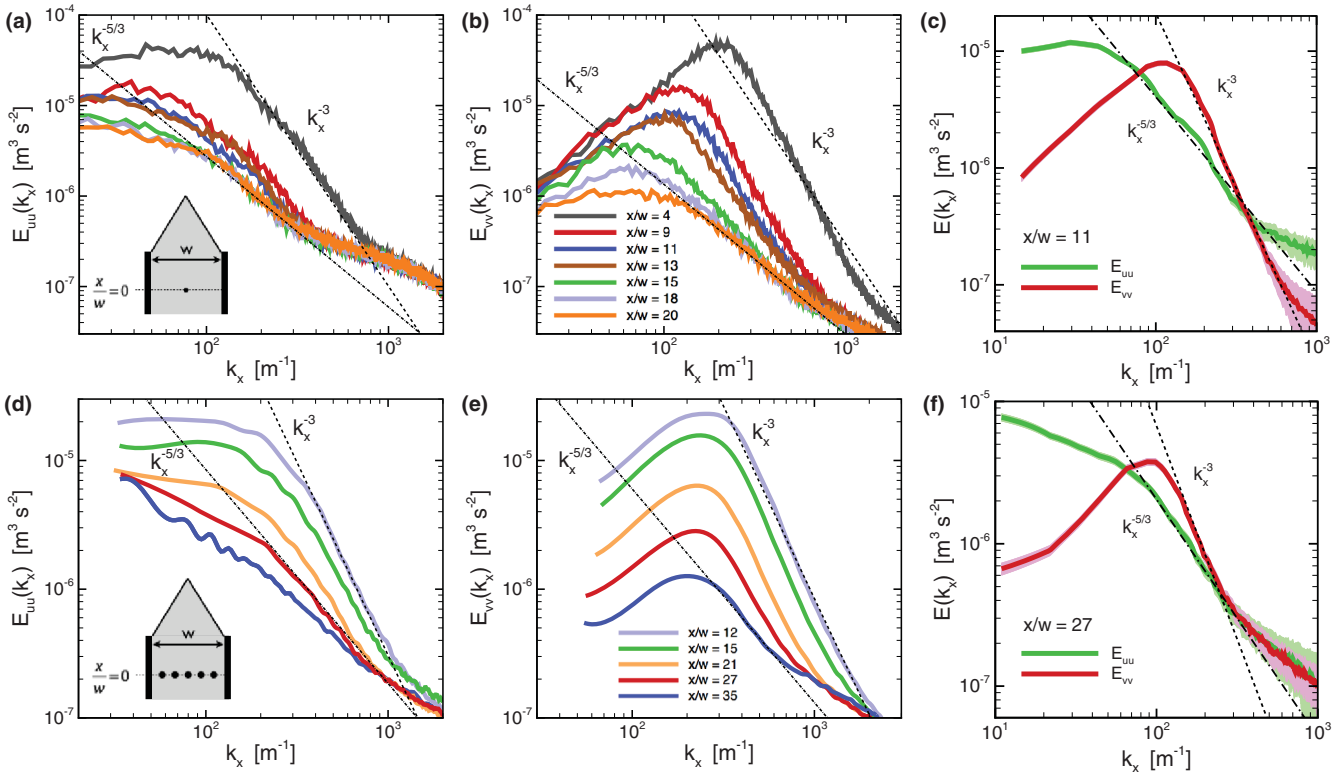

FIG. 3. Route to the Janus spectra in turbulence induced by one rod (a)–(c) and comb (d)–(f) (also, see the Supplemental Material [14] Figs. S-3 and S-4). One rod: The soap film ($w = 23$ mm) is pierced at the center line with a rod of diameter 0.5 mm; the mean velocity at the center line spans 2.10–2.40 m/s. Comb: The soap film ($w = 17$ mm) is pierced symmetrically about the center line with a comb (five rods of diameter 1 mm, spaced 3 mm apart from each other); the mean velocity at the center line spans 2.07–2.60 m/s. (a),(b); (d),(e) The evolution of $E_{uu}(k_x)$ and $E_{vv}(k_x)$ with downstream distance is similar to the case of the two rods (Fig. 2). We show the Janus spectra in (c) for one rod ($x/w = 11$) and in (f) for the comb ($x/w = 27$); the errors (the shaded regions) are negligible in the inertial range. Note that even though the wave number span of the inertial region of $E_{vv}(k_x)$ in (f) is relatively small, we can infer $\alpha_v \approx 3$ by comparing with the energy spectra measured upstream (e). Upstream, α_v is the same, but the span of the inertial region is considerably broader. [Similar considerations also apply to the $E_{vv}(k_x)$ for two rods and one rod.]

enstrophy cascade [6]. Indeed, numerous experiments of soap films flowing downstream of obstacles attest to $\alpha_u \approx \alpha_v \approx 3$ (see, e.g., Ref. [19]).

To interrogate the turbulent flow, we turn to laser Doppler velocimetry (LDV). We use LDV to measure the time series of u and v along the center line of the channel, downstream of the rods and well upstream ($>15w$) of the Marangoni shock [21]. Using Taylor's [22] hypothesis, we transform this time-series data to spatial data in the streamwise direction, from which we compute $E_{uu}(k_x)$ and $E_{vv}(k_x)$. As can be seen from the decrease in the amplitude of the energy spectra [Figs. 2(b) and 2(c)] or from the decay of the turbulent vorticity [Fig. 2(e)], the turbulence decays downstream of the rods. Not far downstream ($x/w \lesssim 10$), $\alpha_u \approx \alpha_v \approx 3$ [Figs. 2(b) and 2(c)], in accord with previous experiments (and also consistent with the initial phase of decaying 2D turbulence without a mean flow). Note that the mechanisms that sustain the direct enstrophy cascade entail strong eddy-eddy interactions [13,23]. Therefore, experiments targeted at the direct enstrophy cascade focus on the region where the eddies have not decayed significantly—the region near the obstacles. Here we depart from these experiments in an unremarkable way: we continue to measure the energy spectra farther downstream. And yet, this unveils a series of remarkable features.

Extrapolating from the later phase of decaying 2D turbulence without a mean flow, downstream of the direct enstrophy cascade we expect steeper energy spectra with $\alpha_u \approx \alpha_v > 3$. The mean flow in the experiment, however, effects a strikingly different fate. (We return to the role of the mean flow later.) For $x/w \gtrsim 12$, α_u begins to decrease but α_v remains ≈ 3 [Figs. 2(b) and 2(c)]. The regime of local isotropy is broken. Farther downstream ($15 \lesssim x/w \lesssim 20$), α_u reaches a plateau $\approx 5/3$, suggesting an unexpected transition to the inverse energy cascade for $E_{uu}(k_x)$. In this region, remarkably, α_v is still ≈ 3, suggesting the persistence of the direct enstrophy cascade for $E_{vv}(k_x)$. That is, over a sizable interval ($\approx 5w$) and over a shared span of wave numbers, $\alpha_u \approx 5/3$ but concurrently $\alpha_v \approx 3$ [Fig. 2(d)]. This is the domain of the Janus spectra. (Even farther downstream, both α_u and α_v decrease

monotonically.) We note, for contrast, that previous experiments in soap-film channels have reported the inverse energy cascade for turbulence forced by rough blades [[8]; Fig. 1(b)]. This roughness-induced turbulent flow exhibits $\alpha_u \approx \alpha_v \approx 5/3$, in accord with local isotropy. Our experiments, on the other hand, have smooth blades, and we find $\alpha_u \approx 5/3$ but without local isotropy $\alpha_u \neq \alpha_v$.

Because the dynamics of decaying 2D turbulence is sensitive to the mode of forcing turbulence [13], we test if the Janus spectra are unique to the nonsymmetric forcing by the two rods. To that end, we conduct experiments with two different obstacles: one rod and comb. (A comb, the standard choice of forcing in soap-film experiments, is a row of rods.) We place the obstacle symmetrically about the center line of the soap-film channel. Proceeding downstream from the obstacle, we first see $\alpha_u \approx \alpha_v \approx 3$; farther downstream, we note that α_u transitions to a plateau $\approx 5/3$ but α_v remains ≈ 3—the Janus spectra (Fig. 3). We conclude that the Janus spectra are a robust phenomenon unaffected by the symmetry (or lack thereof) of the forcing.

The existence of the Janus spectra suggests that the phenomenological theory may be extended to flows without local isotropy. Interestingly, in the Janus spectra, it is not simply that $\alpha_u \neq \alpha_v$, where α_u and α_v assume values whose interpretation necessitates a new theoretical framework. Instead, we find $\alpha_u \approx 5/3$ and $\alpha_v \approx 3$, the same spectral exponents as those predicted by the phenomenological theory for locally isotropic 2D turbulent flows. Based on our empirical results, we postulate a simple generalization of the phenomenological theory for the Janus spectra: the u component transfers energy without dissipation, and the v component transfers enstrophy without dissipation. Consequently, dimensional analysis [3] yields $\alpha_u = 5/3$ and $\alpha_v = 3$.

To seek the physical mechanisms that underlie the Janus spectra, we turn to flow visualization. We illuminate the soap film with monochromatic light (wavelength = 633 nm). The resultant interference fringes render the turbulent eddies visible (Fig. 4; Supplemental Material [14] Fig. S-5). The shapes of the eddies bear witness to the influence of the sheared mean flow in the soap-film channel. Just downstream of the obstacle, the eddies are isotropic [Figs. 4(a) and 4(b)]. Farther downstream, however, the eddies become progressively anisotropic [Figs. 4(c) and 4(d)]. This transition from isotropy to anisotropy—and the accompanying transition from the direct enstrophy cascade to the Janus spectra—can be understood by comparing the magnitudes of the turbulent vorticity and the mean shear.

As the flow evolves downstream, the turbulent vorticity decays, but the mean shear remains roughly the same [see, e.g., Fig. 2(e)]. Upstream, the turbulent eddies prevail. Being relatively unaffected by the mean shear, the locally isotropic flow exhibits the direct enstrophy cascade (similar to the case of decaying 2D turbulence without a mean flow).

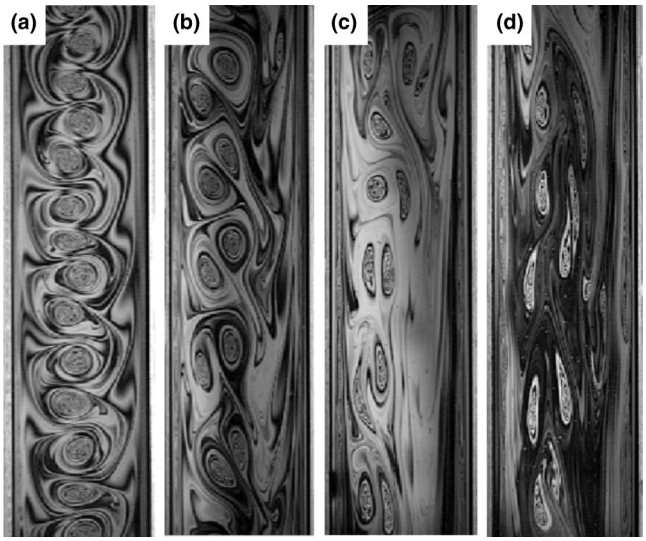

FIG. 4. Turbulent eddies distorted by the sheared mean flow. The soap film ($w = 22$ mm) is pierced at the center line with a rod of diameter 0.5 mm. The mean flow in each panel is from top to bottom; from left to right, the panels document the downstream evolution of the flow: $x/w \approx 1$–4 (a), 6–9 (b), 25–28 (c), and 29–32 (d).

Farther downstream, the turbulent eddies weaken. The weak eddies are distorted by the mean shear [24], as is evident in Figs. 4(c) and 4(d). This effects anisotropy across the scales, large and small. To get to a heuristic picture of the mechanisms that engender the Janus spectra, we proceed by using the shapes of these anisotropic eddies as a guide. Note that the anisotropic eddies of Figs. 4(c) and 4(d) are preferentially elongated along the streamwise direction (also, see Ref. [24]), thereby transferring energy for the u component to larger scales (Supplemental Material [14] Sec. S-5; [25]). We postulate that this energy transfer initiates the inverse energy cascade for the u component. The v component of these anisotropic eddies exhibits different dynamics. Note that the enstrophy flux is modulated by the vorticity gradient [23], which is oriented along v for the streamwise-elongated eddies. We speculate that the v-oriented vorticity gradient sustains the transfer of enstrophy for the v component. These velocity-component-dependent transfers of energy and of enstrophy manifest as the Janus spectra.

While our discussion offers hints about the role of mean shear [26,27], the interaction between mean flow and turbulent vorticity remains poorly understood. This interaction dictates the fate not only of soap-film flows but also of decaying flows in the atmosphere and the ocean, for instance, the waning phase of tropical cyclones. In these quasi-2D decaying turbulent flows that are inextricably embedded in sheared mean flows, anisotropy is but the norm. Our study suggests that the streamwise and transverse fluctuations in these flows partake in mutually independent dynamics and that the tools of the

phenomenological theory can be invoked to predict their behavior. That a theory built assuming local isotropy can still elucidate a manifestly anisotropic turbulent flow strikes us as an extraordinary testament to its generality. In closing, we submit that the study of decaying 2D turbulence embedded in a sheared mean flow is replete with unexpected insights, with implications on a broad range of problems, from the understanding of turbulent cascades to the forecasting of large-scale weather systems.

We thank Gustavo Gioia for helpful discussions and the referees for constructive comments. This work was supported by the Okinawa Institute of Science and Technology Graduate University.

*pinaki@oist.jp

[1] L. F. Richardson, *Weather Prediction by Numerical Process* (Cambridge University Press, Cambridge, 1922), Chap. 4.
[2] A. N. Kolmogorov, Dokl. Akad. Nauk SSSR **30**, 299 (1941) [Proc. R. Soc. A **434**, 9 (1991)]; G. Batchelor, Math. Proc. Cambridge Philos. Soc. **43**, 533 (1947).
[3] In the energy cascade, the eddies transfer energy without dissipation; $E(k)$ depends only on k and ϵ (the rate of energy per unit mass). Dimensional analysis yields $E(k) \sim \epsilon^{2/3} k^{-5/3}$. In the enstrophy cascade, the eddies transfer enstrophy without dissipation; $E(k)$ depends only on k and β (the rate of enstrophy). Dimensional analysis yields $E(k) \sim \beta^{2/3} k^{-3}$.
[4] R. H. Kraichnan, Phys. Fluids **10**, 1417 (1967).
[5] C. Leith, Phys. Fluids **11**, 671 (1968).
[6] G. K. Batchelor, Phys. Fluids **12**, II-233 (1969).
[7] S. Pope, *Turbulent Flows* (Cambridge University Press, Cambridge, England, 2000).
[8] H. Kellay, T. Tran, W. Goldburg, N. Goldenfeld, G. Gioia, and P. Chakraborty, Phys. Rev. Lett. **109**, 254502 (2012); D. Samanta, F. Ingremeau, R. Cerbus, T. Tran, W. I. Goldburg, P. Chakraborty, and H. Kellay, Phys. Rev. Lett. **113**, 024504 (2014).
[9] G. Boffetta and S. Musacchio, Phys. Rev. E **82**, 016307 (2010).
[10] G. D. Nastrom, K. S. Gage, and W. H. Jasperson, Nature (London) **310**, 36 (1984).
[11] Direction-dependent spectral exponents, albeit only with large-to-small-scale cascade transfers, have been observed in space plasma turbulence; see T. Horbury, R. Wicks, and C. Chen, Space Sci. Rev. **172**, 325 (2012).
[12] J. C. McWilliams, J. Fluid Mech. **146**, 21 (1984).
[13] G. Boffetta and R. E. Ecke, Annu. Rev. Fluid Mech. **44**, 427 (2012).
[14] See the Supplemental Material at http://link.aps.org/supplemental/10.1103/PhysRevLett.117.114502, which includes Refs. [15–18], for ancillary figures and discussion.
[15] W. K. George, Jr., P. D. Beuther, and J. L. Lumley, in *Proceedings of the Dynamic Flow Conference 1978 on Dynamic Measurements in Unsteady Flows* (Springer, New York, 1978), pp. 757–800.
[16] R. Adrian and C. Yao, Exp. Fluids **5**, 17 (1986).
[17] P. Vorobieff, M. Rivera, and R. E. Ecke, Phys. Fluids **11**, 2167 (1999).
[18] G. Comte-Bellot and S. Corrsin, J. Fluid Mech. **25**, 657 (1966).
[19] H. Kellay and W. I. Goldburg, Rep. Prog. Phys. **65**, 845 (2002); B. K. Martin, X. L. Wu, W. I. Goldburg, and M. A. Rutgers, Phys. Rev. Lett. **80**, 3964 (1998); M. K. Rivera, H. Aluie, and R. E. Ecke, Phys. Fluids **26**, 055105 (2014).
[20] M. Rutgers, X. Wu, and W. Daniel, Rev. Sci. Instrum. **72**, 3025 (2001).
[21] T. Tran, P. Chakraborty, G. Gioia, S. Steers, and W. Goldburg, Phys. Rev. Lett. **103**, 104501 (2009).
[22] G. I. Taylor, Proc. R. Soc. A **164**, 476 (1938); A. Belmonte, B. Martin, and W. I. Goldburg, Phys. Fluids **12**, 835 (2000).
[23] S. Chen, R. E. Ecke, G. L. Eyink, X. Wang, and Z. Xiao, Phys. Rev. Lett. **91**, 214501 (2003).
[24] S. Kida, J. Phys. Soc. Jpn. **50**, 3517 (1981); P. S. Marcus, J. Fluid Mech. **215**, 393 (1990); S. Toh, K. Ohkitani, and M. Yamada, Physica (Amsterdam) **51D**, 569 (1991); J. Nycander, J. Fluid Mech. **287**, 119 (1995); P. F. Cummins and G. Holloway, J. Fluid Mech. **657**, 394 (2010).
[25] In 3D turbulent shear flows, the interaction between the turbulent fluctuations and the mean shear injects energy in the u component via the "lift-up effect." See, e.g., L. Brandt, Eur. J. Mech. B **47**, 80 (2014). A 2D analog of the lift-up effect may enhance the energy of the u component and thereby aid its transition to the inverse energy cascade.
[26] L. Biferale, I. Daumont, A. Lanotte, and F. Toschi, Phys. Rev. E **66**, 056306 (2002); L. Biferale and I. Procaccia, Phys. Rep. **414**, 43 (2005).
[27] Note that a vertical mean shear transforms a 3D turbulent flow to a 2D turbulent flow on a horizontal plane. See H. Xia, D. Byrne, G. Falkovich, and M. Shats, Nat. Phys. **7**, 321 (2011); D. Byrne and J. A. Zhang, Geophys. Res. Lett. **40**, 1439 (2013). Our results suggest that an in-plane mean shear sunders a 2D decaying turbulent flow into two mutually independent fields of disparate dynamics.